SOFT ROBOTICS
Volume 8, Number 1, 2021

DOI: 10.1089/soro.2019.0137

SoRo
Soft Robotics

ORIGINAL ARTICLE

Untethered-Bioinspired Quadrupedal Robot Based on Double-Chamber Pre-charged Pneumatic Soft Actuators with Highly Flexible Trunk

Yujia Li,[1,*] Tao Ren,[1,*] Yunquan Li,[2] Qingyou Liu,[3] and Yonghua Chen[2]

Abstract

Given that mobile soft robots are adaptable to the environment, they are always tethered with slow locomotion speed. Compared with other types of mobile robots, mobile soft robots may be more suitable for rescuing tasks, accompanying elderly people, and being used as a safe toy for children. However, the infinite freedom of soft robots increases the difficulty of precision control. In addition, the large volume and long tube of the conventional soft actuator structure limit the range of motion of current mobile soft robots. In this article, a newly designed innovative untethered-bioinspired quadrupedal robot based on double-chamber pre-charged pneumatic (DCPCP) soft actuators with highly flexible trunk is proposed. Asymmetrical cross-tendons actuated by servo motors are used to drive the DCPCP soft legs so that buckling can be avoided and mimic the gait of quadruped animals with the simplest drive and control strategy. In addition, the proposed design greatly improves energy efficiency and exhibits superior performance of variable stiffness. The bioinspired highly flexible trunk is designed with the supporting spine structure and tendon driven muscle to deform, which can constantly adjust to the contact situation between the foot and the ground to adjust the center of gravity of the soft quadruped robot and increase stability when walking and turning. The proposed soft quadruped robot does not require any air compressors, valves, and hoses. The characteristics of untethered, high-energy efficiency, linear control, and stability make the soft quadruped robot suitable for many applications.

Keywords: pre-charged pneumatics, double chamber, controllable flexible trunk, untethered, soft robotics

Introduction

QUADRUPED MAMMALS HAVE FLEXIBLE LIMBS, which help them obtain food, escape predators, and adapt to different habitata.[1] Quadruped robots mimic quadruped mammals to enter extreme environmental and hazardous structures instead of human beings, as well as enter the space that humans cannot reach, to expand humans' exploration ability.[2–4] To improve the flexibility and adaptability of quadruped robots to the unpredictable environment, there is much research, that is, elastically suspended loads increase the efficiency of locomotion and load carrying[5]; increasing the freedom of the joints[6,7]; rigid linkages active driven rigid spine[8]; rigid linkages imitate trunk twist[9]; cable-driven leaf spring trunk[10,11]; cable-driven flexible trunk[12]; and cable-driven rigid modular spine.[13] However, the aforementioned robot trunk or legs are mostly made of a rigid structure that does not reflect the elastic supporting role of the muscles, and it can hardly absorb impact energy. The external disturbance has significant influence on the stability of the robot motion. The structural complexity also increases the difficulty of control.

In recent years, research on soft quadruped robots shows that the characteristics of obtaining gentle and safe interactions with the human and environment, adaptability, and energy harvesting provide a strong boost to the development of quadruped robots.[14] Bioinspired soft quadruped robots reflect a remarkable advantage over rigid quadruped robots:

[1]College of Nuclear Technology and Automation Engineering, Chengdu University of Technology, Chengdu, China.
[2]Department of Mechanical Engineering, University of Hong Kong, Hong Kong, China.
[3]State Key Laboratory of Oil and Gas Reservoir Geology and Exploitation, Chengdu University of Technology, Chengdu, China.
*These authors contributed equally to this work.

Energy harvesting could be obtained by exploiting compliant elements of the system; compliance reduces the external disturbances without the need for feedback control to realize complex dexterous locomotion.[15] Typical research in this area includes: fully flexible robot with or without cable,[16–19] robot with rigid body and elastic/flexible legs,[20–23] and jumping robot combined with pneumatics and explosives.[24] However, most of the conventional soft quadruped robots are peristaltic walking or crawling whose motion velocity is slow; controlling the motion of soft robots when using pneumatic actuators driven by chemical reactions is difficult.[25–29] What is more, most soft walking robots require heavy air compressors, valves, and control systems. Several air hoses or wires are connected between the auxiliary equipment and the robot, thereby limiting the flexibility and range of motion of soft robots. In Ref.[30] a pneumatic soft robot is placed on a rigid robot platform and moves to the designated position to perform the task. The robot is equipped with micro-compressors and valves, and the range of motion remains restricted due to the limitations of the hoses.

In the authors' previous research, a pre-charged pneumatic (PCP) soft actuator was proposed.[31] On this basis, a self-pumping soft actuator is developed without a cable, long hoses, and an air compressor. The self-pumping soft actuator design improved supporting stiffness and driving efficiency.[32] However, a self-pumping soft actuator with an equal cross-section and wall thickness proposed by the authors in previous research buckles when pulling the tendon on one side, which may bring structure instability for the quadruped robot legs.

Inspired by the quadruped mammals and based on the authors' previous studies, an untethered-bioinspired quadrupedal robot based on double-chamber pre-charged pneumatic (DCPCP) soft actuators with tendon-driven flexible trunk twisting motion is proposed in this study. The proposed asymmetrical cross-tendon design helps mimic the posture of the dog's leg when stepping forward, as well as changing the posture of the foot; thus, the stability of motion can be enhanced. The adaptive and compliant capability of the soft legs reduces the difficulty of control system and avoids the complex dynamics control used by rigid robots. Bioinspired spine-muscle-trunk twisting enhances the body's flexibility and improves the motion stability. In summary, the proposed untethered-bioinspired quadrupedal robot has smaller weight, better safety, and higher environmental adaptability than a traditional rigid quadruped robot. The soft quadruped robot proposed in this study is expected to accompany elderly people and to be used as a safe toy for children. This research is expected to bring new ideas for the future research of walking robots.

The major contributions of this study are summarized as follows:

1. The proposed bioinspired DCPCP soft leg with variable section and wall thickness has no buckling, which enhances structural stability.
2. The proposed asymmetrical cross-tendon driving makes the soft leg S-shaped and I-shaped with the simplest driving strategy, which approximately simulates the walking posture of a real animal's legs.
3. The proposed bioinspired trunk is designed with the supporting spine structure and tendon-driven muscle to deform, which has a strong supporting ability and high flexibility.

Mechanical Design of the Bioinspired Soft Quadruped Robot

The untethered soft quadruped robot carries the power supply itself; thus, high energy efficiency is needed to effectively accomplish tasks. In addition, soft quadruped robots should own flexibility and a large range of motion. Inspired by the gait of canines as shown in Figure 1a, a soft quadruped robot with four DCPCP soft legs is designed and fabricated as shown in Figure 1b. The total length, width, and height of the robot are 385, 215, and 335 mm, respectively. The soft quadruped robot's legs are pre-charged and do not require hoses, valves, and air compressors. The untethered soft quadruped robot has batteries that are easy to move and are installed in its body. It also has a wider range of motion than a cabled robot.

As shown in Figure 1c, the soft actuator with an equal cross-section and wall thickness proposed by the authors in previous research buckles when pulling the tendon on one side, which may bring structure instability for the quadruped robot legs. The DCPCP soft actuator with a variable cross-section and equal wall thickness avoids the buckling when pulling the tendon on one side, but the end of the actuator tilts up seriously, which is different from the real foot posture of quadruped animals (i.e., canines). In this study, the proposed DCPCP soft leg with a variable section and wall thickness has no buckling. The end of the soft leg tilts slightly. The novel asymmetric cross-tendon driving mode enables the DCPCP soft actuator to simulate the gait of quadruped animals with the simplest drive and control strategy (linear control). Therefore, the stride length of the soft quadruped robot can be increased; the stability of motion can be enhanced.

Figure 1d illustrates a three-dimensional (3D) model of the DCPCP soft leg. The leg is made of three materials, namely silicone rubber, non-woven fabric, and fiber. The length of the DCPCP soft leg is 163 mm. To imitate the legs of real dogs, the diameter of the leg gradually decreases from top to bottom; hence, the largest and smallest diameters of the leg are 60 and 40 mm, respectively. To make the legs S-shaped during cross-tendon driving, the soft legs are designed to be thicker at the top and thinner at the bottom, which is conducive to increasing the stiffness of the thighs and bending the shanks. The two pre-charged chambers of the leg are connected. An inextensible layer made of a soft nonwoven fabric is sandwiched between the two chambers. It makes the soft leg's lateral stiffness greater than the fore and rear stiffness, helping the leg to maintain lateral stability and making it less prone to falling. A fibrous layer between the inner surface of the chamber and the outer surface of the actuator limits the leg expansion in the circumferential direction. The actuation tendons are asymmetrically arranged on both sides of the actuator chamber. The length of the two actuation tendons on both sides can be controlled linearly to adjust the bending direction and displacement of the DCPCP soft actuator. The soft leg is driven by a servo motor (produced by Hangzhou Zhongling Technology Co., Ltd.) through the tendon camera to a horizontal displacement of +100 and −80 mm, as shown in Figure 1e. Compared with conventional air compressors, valves, and hoses, the motor control is small and light, making soft quadruped robots convenient to carry around. Given that the fore and rear sides of the leg can be controlled to bend by the actuation tendon,

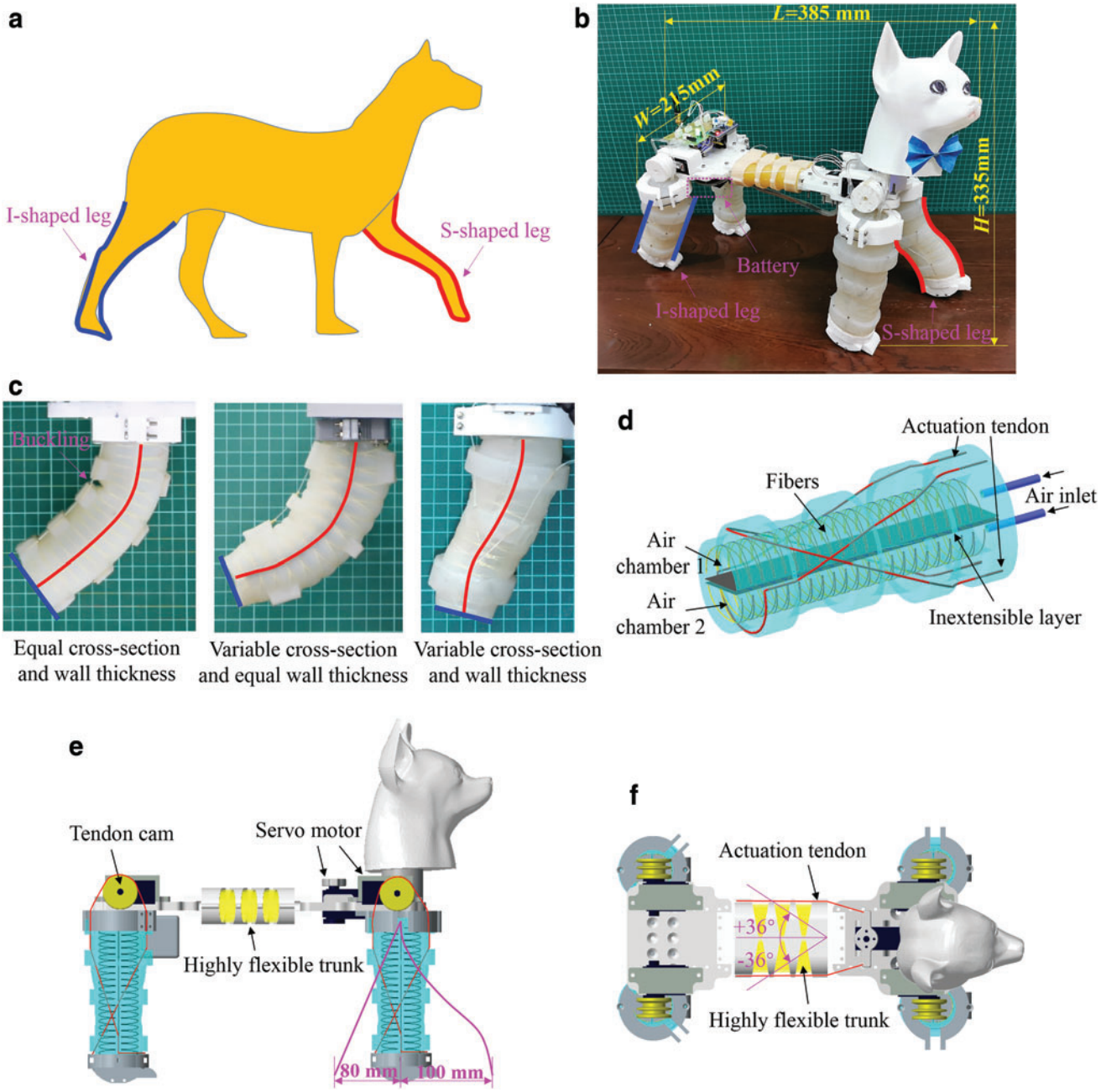

FIG. 1. 3D model of the untethered-bioinspired quadrupedal robot. **(a)** The gait of canines. **(b)** Prototype. **(c)** Comparison among three shapes of different DCPCP soft actuators. **(d)** 3D model of the DCPCP soft leg. **(e)** Side view. **(f)** Top view. 3D, three-dimensional; DCPCP, double-chamber pre-charged pneumatic. Color images are available online.

the stride is larger than the single-chamber pre-charged pneumatic (SCPCP) soft actuator as previously proposed by the authors.

To simulate a real dog's motion, a highly flexible trunk is designed to be twisted. The bioinspired trunk is designed with the supporting spine structure and tendon-driven muscle to deform. The spine and rib are 3D printed with thermoplastic urethane (TPU) that can twist left and right, and they have certain supporting functions in the vertical direction. The pre-charged rubber tube is embedded in the rib, which acts as the muscle to support the spine elastically. Nylon wires act as tendons to drive the trunk to twist. The servo motor drives the nylon wires on both sides of the spine to control the direction and angle of the flexible trunk. The soft quadruped robot's trunk can be twisted from −36° to +36°, as shown in Figure 1f. Twisting of the trunk has the following advantages: (1) a balanced and stable motion, (2) a large step taken when walking straight, and (3) an increased flexibility during turning and not falling easily.

Kinematic Analysis of the Soft Quadruped Robot

The bending angle of the soft quadruped robot leg is linearly controlled by the displacement of the actuation tendon actuated by the servo motors. The bending angle of the flexible trunk is controlled by the rotational angle of the servo

motor. Figure 2 shows the contrast between the twisted and nontwisted trunk when the soft quadruped robot walks straight forward. When the trunk is not twisted as shown in Figure 2a, the step taken is S_1. When the trunk is twisted, the coordinates of the thigh root will be advanced. The trunk twisting is regarded as the transport motion; the step of the foot relative to the thigh root is regarded as the relative motion; and the superposition of the two is the absolute motion of the foot, that is, the stride. Figure 2b shows that the twisting of the trunk moves the step to S_2, which greatly increases the walking speed of the soft quadruped robot.

Figure 2c shows the kinematic model of the soft quadruped robot. Figure 2d shows the initial state of the DCPCP soft leg. When stepping forward, the motor pulls the red actuation tendon to make the leg bend into S-shape. When kicking backward, the motor pulls the yellow actuation tendon to make the leg become I-shape. Figure 2e, f shows the analytical model of the S-shaped DCPCP soft leg. $\widehat{DA_1A_2}$ is the neutral layer of the soft leg, which is made of inextensible and flexible nonwoven fabric. As the leg is S-shaped when stepping forward, the neutral layer is divided into a 67.5 mm-long upper layer and a 45 mm-long lower layer. The upper and lower distances from the actuation tendon to the neutral layer are 28 and 24 mm, respectively. The actuation tendon is tilted in the prototype to generate an S-shaped leg. The total length of the tilt actuation tendon is ΔL, which contains the upper length ΔL_1 and the lower length ΔL_2. We define the total length of the straight actuation tendon as x, which contains the upper length x_1 and the lower length x_2. The bending angle of the upper soft leg is θ_1, and the bending radius of the upper soft leg is $A_1M_1 = r_1$. From the arc length formula, we have

$$\begin{cases} \Delta L_1 = \frac{x_1}{\cos 19^\circ} \\ 67.5 = \theta_1 \times r_1 \\ 67.5 - x_1 = \theta_1 \times (r_1 - 28) \end{cases} \tag{1}$$

Based on Equation (1), the relationship between the upper length of the actuation tendon and the upper bending angle can be obtained. Thus, the stride A_1B_1 of the upper leg and the stride A_1B_2 of the lower leg are

$$A_1B_1 = r_1(1 - \cos\theta_1) = \frac{1999}{\Delta L_1}[1 - \cos(0.03\Delta L_1)] \tag{2}$$

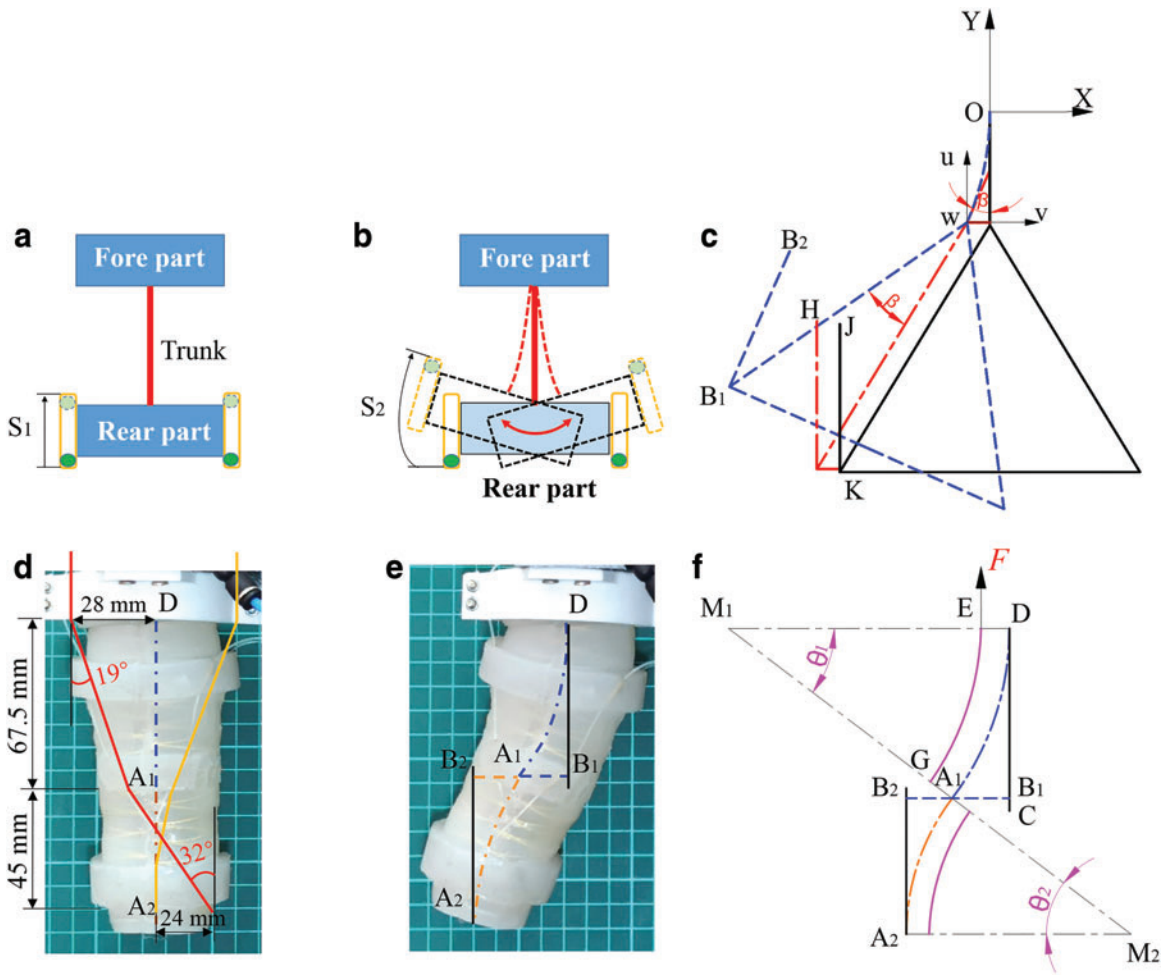

FIG. 2. Diagram and kinematic model of the soft quadruped robot. **(a)** Diagram without trunk twisting. **(b)** Diagram with trunk twisting. **(c)** Kinematic model of the soft quadruped robot. **(d)** Initial state of the DCPCP soft leg. **(e)** S-shaped DCPCP soft leg. **(f)** Analysis model of the S-shaped DCPCP soft leg. Color images are available online.

$$A_1B_2 = \frac{1274}{\Delta L_2}[1 - \cos(0.04\Delta L_2)] \tag{3}$$

The relative motion displacement of the foot is B_1B_2, which equals to JK.

Thus, we can derive the relationship between the pulling speed of the actuation tendon and the bending angular speed of the soft leg by applying differential calculation:

$$v = \frac{28\omega_1}{\cos 19^\circ} + \frac{24\omega_2}{\cos 32^\circ} \tag{4}$$

Let us assume that the soft quadruped robot does not move in the fore part, and the trunk bends to drive the rear part to twist. The length of the flexible trunk is $\widehat{ow} = 76\ mm$. The bending angle of the flexible trunk is β. The distance from the actuation tendon to the neutral layer of the flexible trunk is 20 mm. Thus, the relationship between the length ΔL_3 of the actuation tendon and the bending angle of the flexible trunk is

$$\Delta L_3 = 20\beta \tag{5}$$

Point O at which the fore part connected to the flexible trunk is the origin in establishing the global coordinate system XOY. Point w at which the rear half body connected to the flexible trunk is the origin to establish the motion coordinate system uwv. The motion of the foot is translated to the motion coordinate system and then rotated around point w of the motion coordinate system. Therefore, the translation matrix of the motion coordinate system relative to the global coordinate system can be obtained:

$${}^{O}T_w = \begin{bmatrix} 1 & 0 & 0 & -\frac{76}{\beta}(1-\cos\beta) \\ 0 & 1 & 0 & -\frac{76}{\beta}\sin\beta \\ 0 & 0 & 1 & 0 \\ 0 & 0 & 0 & 1 \end{bmatrix} \tag{6}$$

The position of point H in the motion coordinate system is

$${}^{w}P_H = [\ -66 \quad -76 + B_1B_2 \quad 0 \quad 1\ ]^T \tag{7}$$

The rotation matrix from point B_2 to point H in the motion coordinate system is

$${}^{H}R_{B_2} = \begin{bmatrix} \cos\beta & \sin\beta & 0 & 0 \\ -\sin\beta & \cos\beta & 0 & 0 \\ 0 & 0 & 1 & 0 \\ 0 & 0 & 0 & 1 \end{bmatrix} \tag{8}$$

We can derive the coordinate of point B_2 in the global coordinate system:

$$\begin{aligned} {}^{O}P_{B_2} &= {}^{O}T_w\,{}^{H}R_{B_2}\,{}^{w}P_H \\ &= \begin{bmatrix} (B_1B_2-76)\sin\beta + \left(\frac{76}{\beta}-66\right)\cos\beta - \frac{76}{\beta} \\ (B_1B_2-76)\cos\beta - \left(\frac{76}{\beta}-66\right)\sin\beta \\ 0 \\ 1 \end{bmatrix} \end{aligned} \tag{9}$$

The coordinate of point K and J in the global coordinate system can be obtained from the structural dimensions:

$${}^{O}P_K = [\ -66 \quad -152 \quad 0 \quad 1\ ]^T \tag{10}$$

$${}^{O}P_J = [\ -66 \quad -152 + B_1B_2 \quad 0 \quad 1\ ]^T \tag{11}$$

Finally, the incremental step of trunk twisting is obtained compared with that of trunk nontwisting:

$$\begin{aligned} {}^{O}Y_{B_2} - {}^{O}Y_J = &\left(66 - \frac{76}{\beta}\right)\sin\beta + (B_1B_2 - 76)\cos\beta \\ &- B_1B_2 + 152 \end{aligned} \tag{12}$$

The step of trunk twisting is

$${}^{O}Y_{B_2} - {}^{O}Y_K = {}^{O}Y_{B_2} - {}^{O}Y_J + B_1B_2 \tag{13}$$

Experimental Test of the Soft Leg and Quadruped Robot

To verify the performance advantages of the DCPCP soft actuator and the feasibility of bioinspired bending DCPCP soft actuator in locomotion, a series of experiments are carried out in this research. An experimental platform was designed, as shown in Figure 3a. One end of the actuation tendon is connected to the end of the soft actuator, whereas the other end is connected to the force sensor mounted on the linear guide. The linear guide moves at a uniform speed of 50 mm/min and pulls the tendon to bend the DCPCP soft actuator; the soft actuator is charged with different air pressures of 10, 20, 30, and 40 kPa. Two pressure sensors (MT-802 series pressure sensor produced by Yaohu Electronic Technology Co., Ltd. with accuracy of 0.5% full-scale [FS]) are connected to the two chambers of the DCPCP soft actuator to measure the air pressure variation during actuator bending. A camera is used to capture the deformation state during actuation. The bending angles and the horizontal displacements of the actuator in various states are measured by importing the images into the AUTOCAD software. All the experiments were conducted at least three times at room temperature to ensure the repeatability.

Comparison of SCPCP and DCPCP soft actuators

To compare the driving performance of SCPCP and DCPCP soft actuators, we designed an SCPCP soft actuator with the same chamber volume as the DCPCP soft actuator. The difference is that the SCPCP soft actuator's inextensible layer is placed on one side of the arc surface of the actuator to limit the elongation of the actuator on this side. The fiber layer limits the expansion of the actuator in the radial direction. When the actuator is filled with compressed air, it immediately produces a bending motion. Figure 3b and c show the experiment setups of the SCPCP and DCPCP soft actuators.

Air pressure ranging from 10 to 40 kPa was charged into the two actuators. Under each pressure, tensile force was increased from 0 to 20 N, observing and recording the bending angles of the two actuators. Figure 4a shows that the DCPCP soft actuator has a larger range of bending angles compared with the SCPCP soft actuator under the same air pressure,

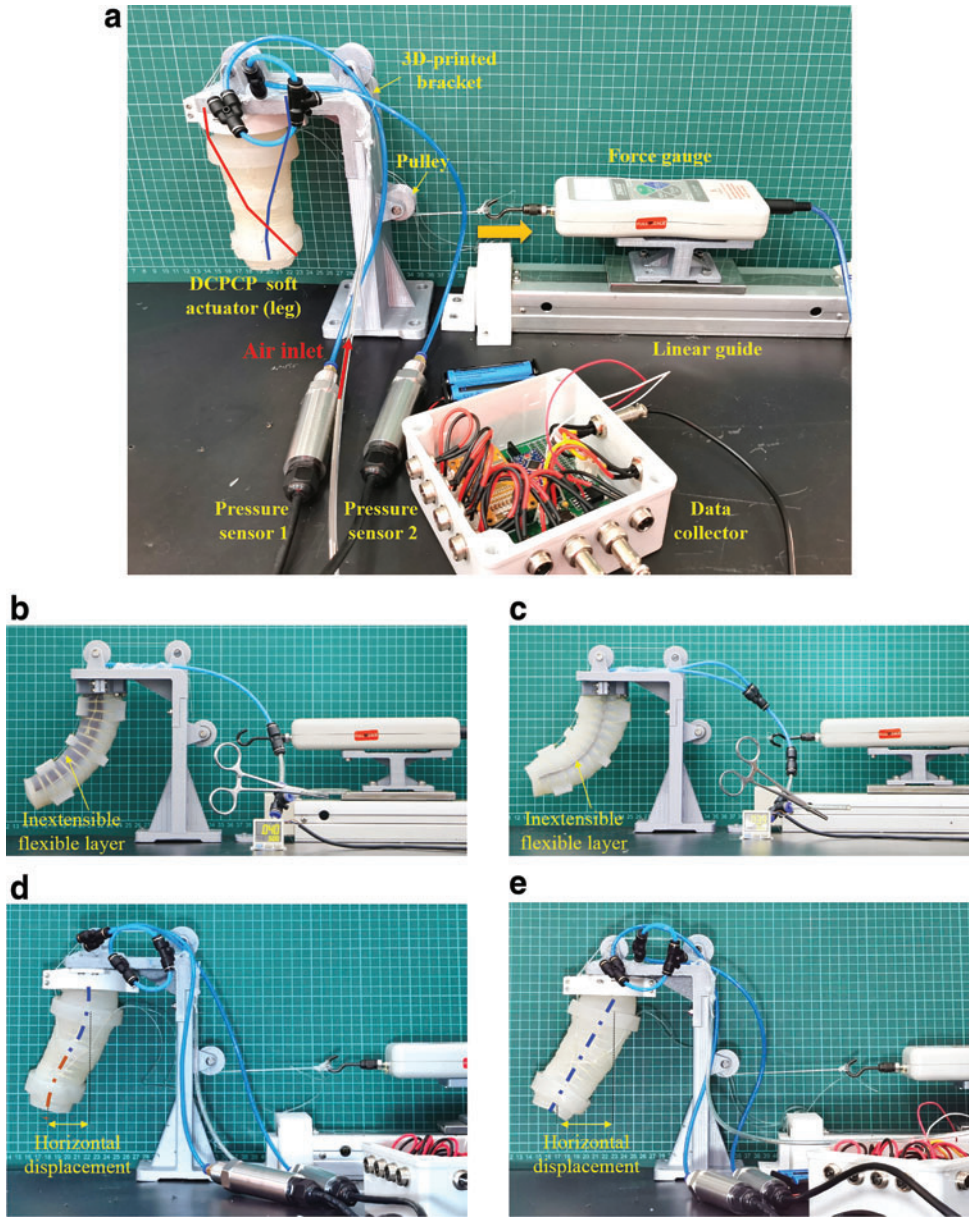

FIG. 3. Force and air pressure experiments of the DCPCP soft actuators/legs. **(a)** Experimental platform. **(b)** J-shaped SCPCP soft actuator. **(c)** J-shaped DCPCP soft actuator. **(d)** S-shaped DCPCP soft leg (*step forward*). **(e)** I-shaped DCPCP soft leg (*kick backward*). Color images are available online.

indicating that its energy efficiency is considerably higher than that of the latter. As shown in Figure 4b, the air pressure (DCPCP-N1 and DCPCP-N2) changes up to 6.33 kPa when the two chambers are disconnected; whereas the air pressure (DCPCP-Y) increases only 0.52 kPa when the two chambers are connected, where DCPCP-N1 and DCPCP-N2 represent the disconnected chambers. DCPCP-Y represents the connected chamber. After pre-charging the DCPCP soft actuator with air, the soft skin on one side is compressed by pulling the actuation tendon; at the same time, soft skin on the other side is stretched. Given the constraint of the inextensible flexible layer, the volume of the side in compression is reduced, causing air to be extruded to the stretched side that has an increased volume. Therefore, the total volume of the DCPCP soft actuator remains almost the same during the actuation process. In the experiment, the elasticity of the silica gel material prevents the volume of the chamber from increasing, so the volume of the connected two chambers is slightly smaller than that in the ideal state. Due to the constraint of one side with an inextensible flexible layer, and soft skin stretch on the other side during bending, the volume of the SCPCP soft actuator increases when bent. The air pressure (in SCPCP) decreases by up to 2.65 kPa during the bending operation.

Figure 4c–f shows that the bending angle and the pulling force of the SCPCP and DCPCP structures are linear, which are extremely advantageous for the control. Under the same air pressure and tension, the bending angle of the actuator is large when the two chambers are connected to each other. Therefore, the actuator in which the two chambers connect with each other under the same air pressure and the same bending angle requires less driving force. As air pressure increases, the actuator's ability to resist bending increases. Thus, the maximum angle at which the actuator can bend decreases. However, after air pressure increases, the actuators in which the two chambers connect with each other exhibit superior performance, and the stiffness mostly changes

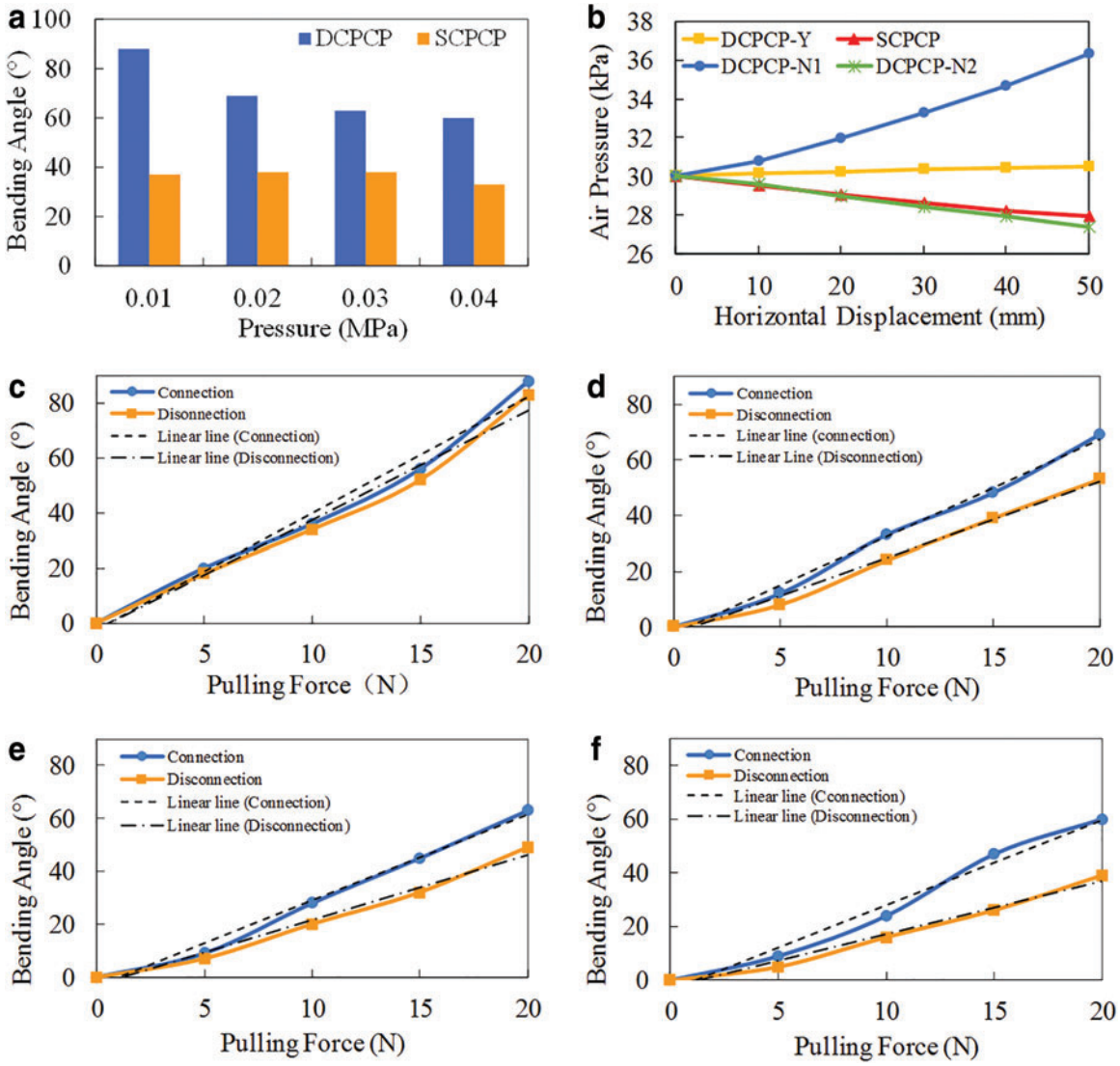

FIG. 4. Comparison of SCPCP and DCPCP soft actuators. **(a)** Driving efficiency. **(b)** Air pressure. **(c)** DCPCP 0.1 kPa. **(d)** DCPCP 0.2 kPa. **(e)** DCPCP 0.3 kPa. **(f)** DCPCP 0.4 kPa. SCPCP, single-chamber pre-charged pneumatic. Color images are available online.

in the same pulling force range. This feature helps the actuator to improve energy efficiency, making it extremely easy to apply to untethered PCP soft robots.

In summary, the total volume of the actuator remains almost the same when the two chambers are connected to each other. Excess air is only pressed from one chamber to the other; hence, air pressure changes minimally. The pulling force produced by the servo motor is almost entirely used to bend the soft actuator without wasting excess energy on the friction loss of the compressed air. However, the volume on the compression side of the disconnected structure decreases substantially and air pressure increases rapidly. A portion of the servo motor is used to compress air in the chamber so that energy efficiency is not as high as the structure in which the two chambers are connected.

Performance test of the bioinspired DCPCP soft leg

To obtain the leg motion performance of the bioinspired DCPCP soft leg, the changes of pulling force and air pressure with the horizontal displacement were tested in the experiments, as shown in Figure 3d and e. Figure 3d shows the S-shaped DCPCP soft leg when walking forward. Figure 3e shows the I-shaped DCPCP soft leg when kicking backward. Figure 5 shows the test results of the bioinspired DCPCP soft legs. From Figure 5a–d, when pulling the end of the DCPCP soft legs to the same horizontal displacement, the pulling force of the disconnected DCPCP is larger than that of the connected DCPCP. This result corresponds to the experiments and analysis in the Comparison of SCPCP and DCPCP Soft Actuators section. The pulling force increases with the increase of pre-charged air pressure. However, the influence of pre-charged air pressure on pulling force is not obvious. The reason is that the axial deformation of the DCPCP soft leg occurs during the pulling process, so the influence of the elasticity of the structure on the pulling force is greater than that of the air pressure to some extent. When the soft leg is bent into S-shape by the cross-actuation tendon, it needs to be bent twice; however, it only needs to be bent once when the

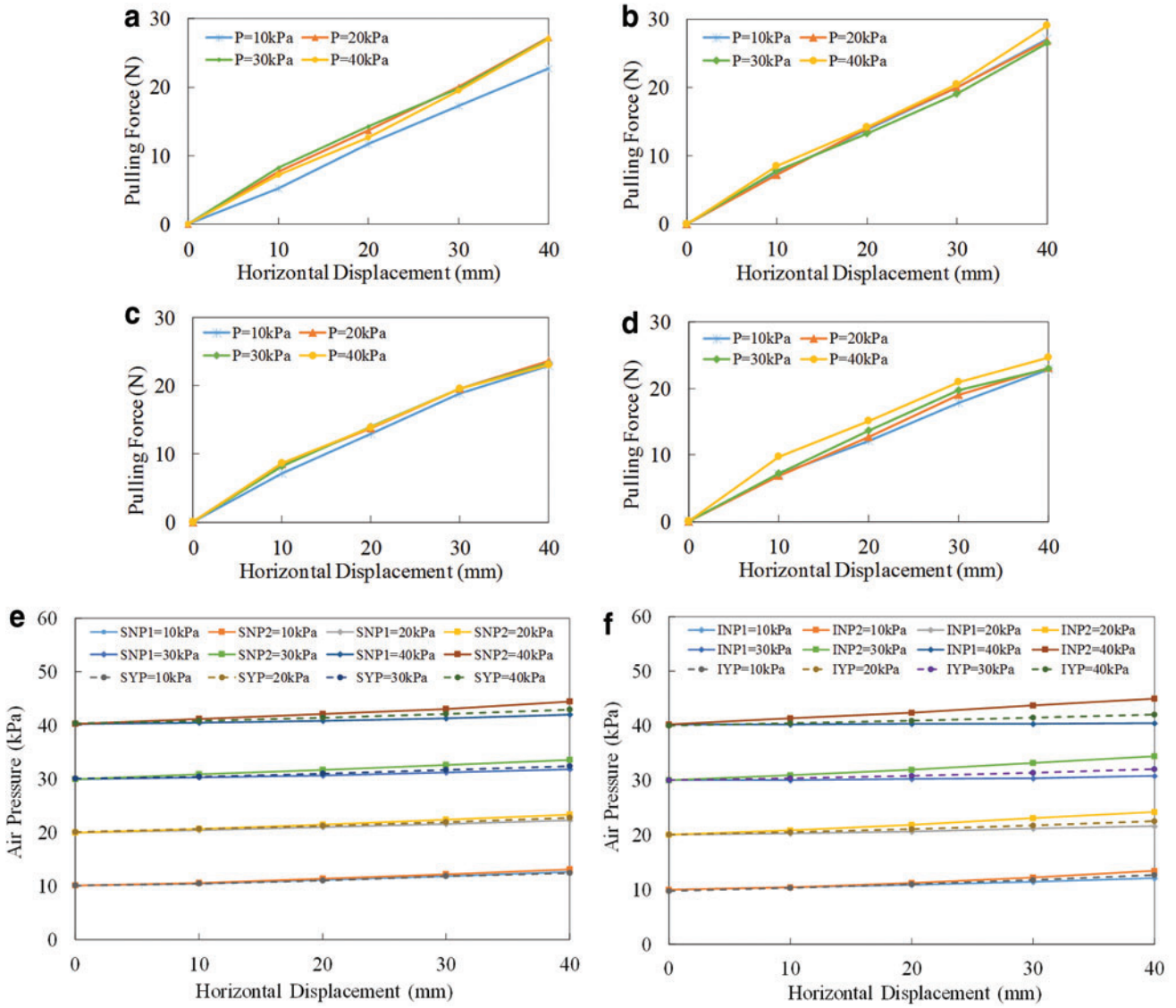

FIG. 5. Performance test of the bioinspired DCPCP soft leg. **(a)** S-shaped connected DCPCP. **(b)** S-shaped disconnected DCPCP. **(c)** I-shaped connected DCPCP. **(d)** I-shaped disconnected DCPCP. **(e)** S-shaped DCPCP. **(f)** I-shaped DCPCP. INP, pressure of I-shaped disconnected DCPCP; IYP, pressure of I-shaped connected DCPCP; SNP, pressure of S-shaped disconnected DCPCP; SYP, pressure of S-shaped connected DCPCP. Color images are available online.

leg is deformed into I-shape. Therefore, the pulling force of the S-shaped DCPCP soft leg is larger than that of the I-shaped DCPCP soft leg.

As shown in Figure 5e and f, the air pressure in the DCPCP soft leg increases with the increase of the horizontal displacement. The air pressure increase range of the connected DCPCP soft leg (the pressure of S-shaped connected DCPCP [SYP] or the pressure of I-shaped connected DCPCP [IYP]) is in the middle of the air pressure range of the two disconnected DCPCP chambers (the pressure in air chamber 1 of S-shaped disconnected DCPCP [SNP1] and the pressure in air chamber 2 of S-shaped disconnected DCPCP [SNP2]; or the pressure in air chamber 1 of I-shaped disconnected DCPCP [INP1] and the pressure in air chamber 2 of I-shaped disconnected DCPCP [INP2]). When pulling the actuation tendon, the axial length of the I-shaped DCPCP soft leg is shortened, resulting in the decrease of air chamber volume and the increase of air pressure. Therefore, the air pressure increment of the I-shaped DCPCP soft leg is larger than that of the S-shaped DCPCP soft leg.

Gait implementation on the soft quadruped robot

The soft quadruped robot has five servo motors on the body, four of which control the motion of the four legs and one that controls the bending angle of the elastic 3D-printing trunk. The five servo motors are controlled by a serial bus. The Arduino Nano control board with the processor for the ATmega328P is mounted on the body of the robotic dog. The control program was compiled, which contains the identity document (ID) and position information of the control servo motor. A control signal pulse to the servo motor was sent by the Arduino Nano control board. The rotational angle of the servo motor is determined by the duration of the transmitted

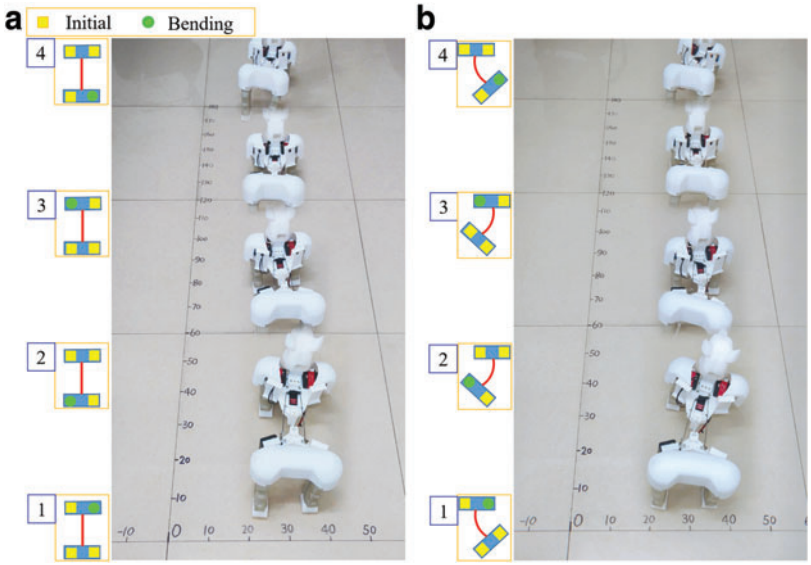

FIG. 6. Linkage-bending elastic 3D-printing trunk twisting effect on walking gait of the soft quadruped robot. **(a)** Walking gait without trunk twisting. **(b)** Walking gait with trunk twisting. 1–4 represent the actuation sequence of four legs, which is RF (right fore) leg-1, LH (left hind) leg-2, LF (left fore) leg-3, and RH (right hind) leg-4. Color images are available online.

control signal pulse, in which the duration of the pulse is from 0.5 to 2.5 ms, and the corresponding rotational angle of the servo motor is 0° to 180°.

Figure 6 shows the walking gait of a quadruped robot with a linkage-bending elastic 3D-printing trunk and a J-shaped bending leg based on the DCPCP soft actuator. The trunk can be twisted to 18° by controlling the servo motor to make the crank-connecting rod move. The actuation tendon displacement of each leg is 15 mm. When the trunk is not twisted, the soft quadruped robot takes 20 steps to walk 120 cm, whereas the soft quadruped robot takes only 16 steps to walk in the same distance with a twisted trunk. The experimental result shows that the torsion of the trunk improves the walking speed of the quadruped robot.

The stride when the trunk is not twisted is calculated by Equation (2) to be 48.65 mm. For J-shaped bending legs, A_1B_2 is 0. The stride when the trunk is twisted is calculated by Equation (13) to be 75.24 mm. The actual stride measured in the experiment is 67.35 mm, and the relative error is 10.5%. The reason for the experimental error is that the experimental ground is smooth and the robot's foot slipped while walking; hence, the actual stride is smaller than the calculated stride. The untethered quadrupedal robot proposed in this study is lighter than the rigid robots and faster than the soft robots, which demonstrates high efficiency and good motion performance.

In addition, the twisting of the trunk makes the soft quadruped robot turn flexible, and the turning radius is smaller than that of the nontwisted scenario. Figure 7 shows the linkage-bending trunk twisting effect on the turning gait of the soft quadruped robot. The diameter of the turning motion with trunk twisting is 96 cm, which is much smaller than that of the turning motion without trunk twisting at 120 cm. The soft quadruped robot without trunk twisting takes 68 steps to turn around, whereas the soft quadruped robot with trunk twisting takes only 49 steps. The experimental results show that trunk twisting increases the turning speed of the soft quadruped robot. When the soft quadruped robot does not twist its trunk, it will easy fall when it moves by gait in achieving the turning motion. However, the soft quadruped robot that twists the trunk almost never falls.

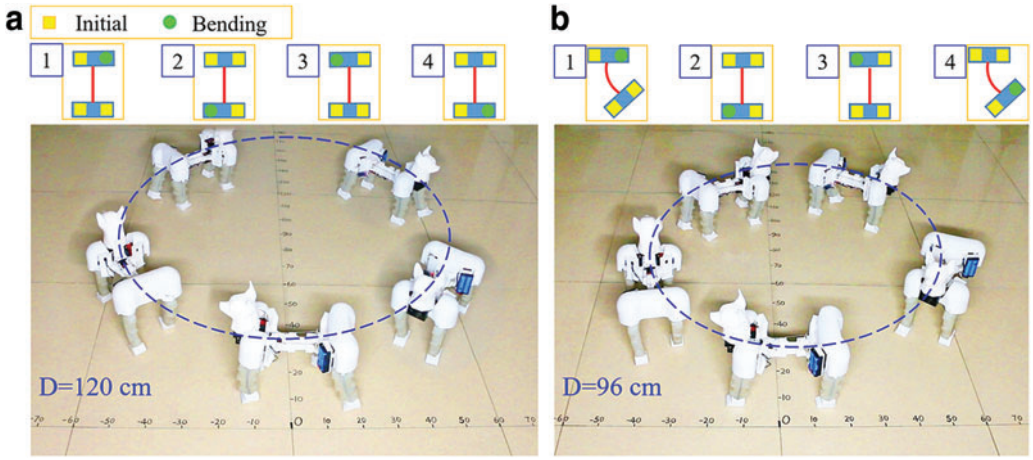

FIG. 7. Linkage-bending elastic 3D-printing trunk twisting effect on turning gait of the soft quadruped robot. **(a)** Turning gait without trunk twisting. **(b)** Turning gait with trunk twisting. 1–4 represent the actuation sequence of four legs, which is RF (right fore) leg-1, LH (left hind) leg-2, LF (left fore) leg-3, and RH (right hind) leg-4. Color images are available online.

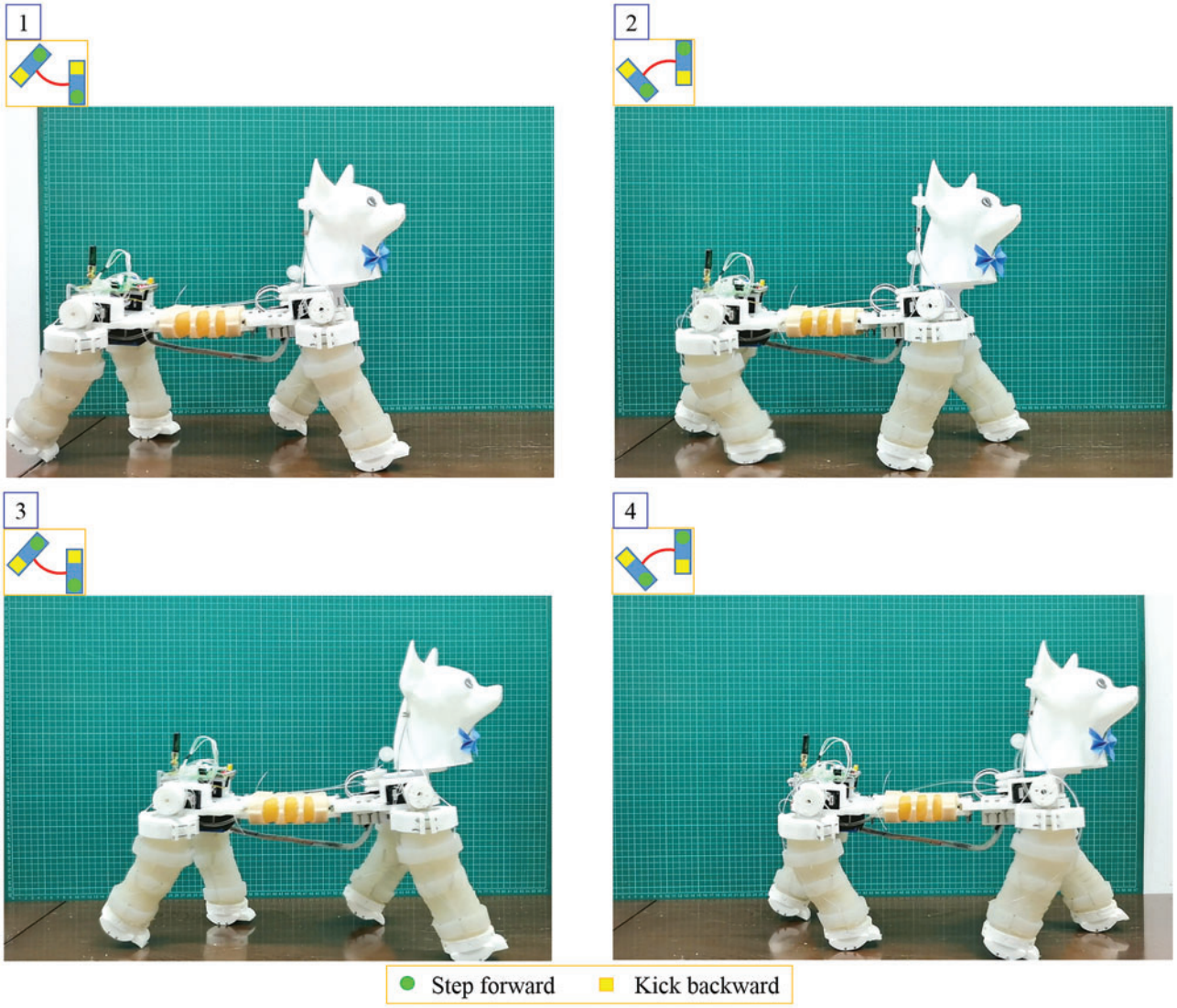

FIG. 8. Tendon-driven highly flexible trunk twisting effect on walking gait of the bioinspired soft quadruped robot. 1–4 represent the actuation sequence of four legs and flexible trunk: (1) RF and LH leg with left bent trunk, (2) LF and RH leg with right bent trunk, (3) RF and LH leg with left bent trunk, (4) LF and RH leg with right bent trunk. Color images are available online.

Therefore, the twisting of the trunk not only reduces the turning radius and increases turning speed, but it also enhances motion stability while turning.

To show the advantages of the proposed bioinspired soft quadruped robot, a group of experiments have been carried out, as shown in Figure 8. The bioinspired soft quadruped robot has five servo motors on the body, four of which control the motion of the four legs and one that controls the bending angle of the flexible spine-muscle trunk. The five servo motors are controlled by a serial bus. The core control board with the processor for the STM32F103C8T6 is mounted on the body of the soft quadruped robot. Personal computer via the serial port sends a motion command, which contains the ID and position information of the control servo motor. The 2.4G wireless module transmits the data to the STM32.

When the novel bioinspired quadrupedal robot steps forward, the leg is bent into S-shape by one of the actuation tendons; when it kicks backward, the leg is changed into I-shape by another actuation tendon. The motor on the trunk drives the actuation tendons to bend the bionic flexible trunk, so that it can cooperate with the leg motion to increase the stride and improve the motion stability. The trunk can be twisted to 36° by controlling the servo motor to pull the actuation tendons. When the trunk is not twisted, the soft quadruped robot takes 8 steps to walk 90 cm, whereas the soft quadruped robot takes only six steps with a twisted highly flexible trunk. The trunk is constantly twisted according to the contact situation between the foot and the ground to adjust the center of gravity of the soft quadruped robot and to increase stability when walking. The video showing the gait implementation on the soft quadruped robot is uploaded as a Supplementary Video S1.

Conclusion

In the authors' previous research, a self-pumping soft actuator with an equal cross-section and wall thickness is proposed. It will buckle when pulling the tendon on one side, which may bring structure instability for the quadruped robot

legs. In this article, a newly designed innovative untethered-bioinspired quadrupedal robot based on DCPCP soft actuators with highly flexible trunk is proposed. The proposed DCPCP soft leg has a variable section and wall thickness so that buckling can be avoided. The proposed asymmetrical cross-tendon driving enables the soft leg deforming in S-shape with the simplest driving strategy, which approximately simulates the posture of a real animal's legs when the quadruped robot steps forward. The end of the soft leg tilts slightly so as to mimic the posture of a real dog's feet. Soft legs are I-shaped when kicking backward and pushing against the ground, helping to push the body moving forward. The locomotion stability of the robot is enhanced. The proposed asymmetrical cross-tendon driving DCPCP soft legs may bring new inspiration for the development of soft quadruped robots.

In addition, almost all the energy of the servo motor driving actuation tendon is used to bend the soft actuator without wasting excess energy on the friction loss of the compressed air. The experimental results show that the DCPCP soft actuator greatly improves energy efficiency compared with the SCPCP soft actuator. After air pressure is increased, the actuators in which the two chambers were connected with each other exhibit superior performance, and the stiffness is mostly changed in the same pulling force range. This feature helped the actuator to improve energy efficiency, making it extremely easy to apply to untethered PCP soft robots.

The bioinspired highly flexible trunk is designed with the supporting spine structure and tendon-driven muscle to deform, which can constantly adjust to the contact situation between the foot and the ground to adjust the center of gravity of the soft quadruped robot and increase stability when walking and turning. The trunk is constantly twisted according to the contact situation between the foot and the ground to adjust the center of gravity of the soft quadruped robot and increase stability when walking. The experimental result shows that the torsion of the trunk not only improves the walking and turning stride and reduces the turning radius, but it also enhances the stability and flexibility of the motion during turning. The untethered-bioinspired soft quadruped robot proposed in this article is expected to be used to accompany elderly people and as a safe toy for children.

Author Disclosure Statement

No competing financial interests exist.

Funding Information

This work was supported in part by the National Natural Science Foundation of China under Project 51805443 and U19A2097, and in part by the Sichuan Science and Technology Program under Project 2019YFG0123.

Supplementary Material

Supplementary Video S1

References

1. Lee DV, Bertram JEA, Todhunter RJ. Acceleration and balance in trotting dogs. J Exp Biol 1999;202:3565–3573.
2. Raibert MH. Trotting, pacing and bounding by a quadruped robot. J Biomech 1990;23:79–98.
3. Raibert M, Blankespoor K, Nelson G, *et al*. BigDog, the rough-terrain quadruped robot. IFAC Proc Vol 2008;41: 10822–10825.
4. Hong M, Yun-Xia L. Walking mechanism and gait design of a novel compound quadruped robot. In: 2018 3rd International Conference on Robotics and Automation Engineering (ICRAE), Guangzhou, China, November 17–19, 2018, pp. 10–13. IEEE.
5. Ackerman J, Seipel J. Energy efficiency of legged robot locomotion with elastically suspended loads. IEEE Trans Robot 2013;29:321–330.
6. Katz B, Di Carlo J, Kim S. Mini Cheetah: A platform for pushing the limits of dynamic quadruped control. In: 2019 International Conference on Robotics and Automation (ICRA), Montreal, QC, Canada, May 20–24, 2019, pp. 6295–6301. IEEE.
7. Yang J, Jia W, Sun Y, *et al*. Mechanical design of a compact and dexterous quadruped robot. In: 2017 IEEE International Conference on Mechatronics and Automation (ICMA), Takamatsu, Japan, August 6–9, 2017, pp. 1450–1456. IEEE.
8. Khoramshahi M, Spröwitz A, Tuleu A, *et al*. Benefits of an active spine supported bounding locomotion with a small compliant quadruped robot. In: IEEE International Conference on Robotics and Automation, Karlsruhe, Germany, May 6–10, 2013, pp. 3329–3334. IEEE.
9. Zhang C, Dai J. Trot Gait with twisting trunk of a metamorphic quadruped robot. J Bionic Eng 2018;15:971–981.
10. Weinmeister K, Eckert P, Witte H, *et al*. Cheetah-cub-S: Steering of a quadruped robot using trunk motion. In: 2015 IEEE international symposium on safety, security, and rescue robotics (SSRR), West Lafayette, IN, October 18–20, 2015, pp. 1–6. IEEE.
11. Cho H, Nishikawa S, Niiyama R, *et al*. Dynamic locomotion of quadruped with laterally parallel leaf spring spine. In: International Conference on Climbing and Walking Robots and the Support Technologies for Mobile Machines, Kuala Lumpur, Malaysia, August 26–28, 2019, pp. 91–98. CLAWAR Association Ltd.
12. Kito Y, Sueoka Y, Nakanishi D, *et al*. Quadruped passive dynamic walking robot with a new trunk structure inspired by spine. In: Proceedings of Dynamic Walking, ETH Zurich, Switzerland, June 10–13, 2014.
13. Sabelhaus AP, van Vuuren LJ, Joshi A, *et al*. Design, simulation, and testing of a flexible actuated spine for quadruped robots. arXiv preprint arXiv 2018;1804.06527.
14. Laschi C, Mazzolai B, Cianchetti M. Soft robotics: Technologies and systems pushing the boundaries of robot abilities. Sci Robot 2016;1: eaah3690.
15. Calisti M, Picardi G, Laschi C. Fundamentals of soft robot locomotion. J R Soc Interface 2017;14:20170101.
16. Majidi C, Shepherd R F, Kramer R K, *et al*. Influence of surface traction on soft robot undulation. Int J Robot Res 2013;32:1577–1584.
17. Tolley MT, Shepherd RF, Mosadegh B, *et al*. A resilient, untethered soft robot. Soft Robot 2014;1:213–223.
18. Morin SA, Shepherd RF, Kwok SW, *et al*. Camouflage and display for soft machines. Science 2012;337:828–832.
19. Cianchetti M, Calisti M, Margheri L, *et al*. Bioinspired locomotion and grasping in water: the soft eight-arm OCTOPUS robot. Bioinspirat Biomim 2015;10:035003.
20. Waynelovich J, Frey T, Baljon A, *et al*. Versatile and dexterous soft robotic leg system for untethered operations. Soft Robot 2016;3:64–70.

21. Drotman D, Jadhav S, Karimi M, *et al*. 3D printed soft actuators for a legged robot capable of navigating unstructured terrain. In: International Conference on Robotics and Automation (ICRA), Singapore, Singapore, May 29–June 3, 2017, pp. 5532–5538. IEEE.
22. Galloway KC, Clark JE, Koditschek DE. Design of a tunable stiffness composite leg for dynamic locomotion. In: International Design Engineering Technical Conferences and Computers and Information in Engineering Conference. American Society of Mechanical Engineers Digital Collection, San Diego, California, USA, August 30–September 2, 2009, pp. 215–222.
23. Zheng T, Godage IS, Branson DT, *et al*. Octopus inspired walking robot: design, control and experimental validation. In: International Conference on Robotics and Automation, Karlsruhe, Germany, 2013, pp. 816–821. IEEE.
24. Tolley MT, Shepherd RF, Karpelson M, *et al.* An untethered jumping soft robot. In: IEEE/RSJ International Conference on Intelligent Robots and Systems, Chicago, IL, September 14, 2014, pp. 561–566. IEEE.
25. Jing Z, Qiao L, Pan H, *et al*. An overview of the configuration and manipulation of soft robotics for on-orbit servicing. Sci China Inform Sci 2017;60:050201.
26. Umedachi T, Vikas V, Trimmer BA. Softworms: The design and control of nonpneumatic, 3D-printed, deformable robots. Bioinspirat Biomim 2016;11:1748–3190.
27. Kitamori T, Wada A, Nabae H, et al. Untethered three-arm pneumatic robot using hose-free pneumatic actuator. In: IEEE/RSJ International Conference on Intelligent Robots and Systems, Daejeon, South Korea, October 9, 2016, pp. 543–548. IEEE.
28. Onal CD, Chen X, Whitesides GM, *et al.* Soft mobile robots with on-board chemical pressure generation. In: Proceedings of International Symposium on Robotics Research, Flagstaff, AZ, USA, August 28–September 1, 2011, pp. 1–16.
29. Daniela R, Tolley M T. Design, fabrication and control of soft robots. Nature 2015;521:467–475.
30. Stokes AA, Shepherd RF, Morin SA, *et al.* A hybrid combining hard and soft robots. Soft Robot 2014;1:70–74.
31. Li Y, Chen Y, Ren T, *et al*. Precharged pneumatic soft actuators and their applications to untethered soft robots. Soft Robot 2018;5:567–575.
32. Ren T, Li YT, Xu M, *et al*. A novel tendon-driven soft actuator with self-pumping property. Soft Robot, 2020;7:130–139.

Address correspondence to:
Tao Ren
College of Nuclear Technology
and Automation Engineering
Chengdu University of Technology
No. 1, East 3rd Road, Erxian Bridge, Chenghua District
Chengdu 610059
China

E-mail: rtone@foxmail.com